

INTERFACIAL WICKING FLOW THROUGH HIERARCHICAL
STRUCTURE OF NATURAL CELLULOSE FIBERS FOR
BIOMEDICAL MICROFLUIDIC DEVICES

SAHBA SADIR

A thesis submitted in fulfilment of the
requirements for the award of the degree of
Doctor of Philosophy (Mechanical Engineering)

Faculty of Mechanical Engineering
Universiti Teknologi Malaysia

NOVEMBER 2015

DEDICATION

To my father's soul for his words of inspiration and encouragement,

I wish he was here to see his dream comes true.

To my beloved mother, for her support and prayers to me,

To my lovely husband for his support and patience,

ACKNOWLEDGEMENTS

In the Name of Allah, the most gracious, the most merciful. First of all thanks to my god for giving me support, guidance, patience and perseverance of my study.

This dissertation would not have been possible without several individuals who were always there to support me to complete the work.

First and foremost, I am very grateful to my supervisor Dr. Dedy H.B Wicaksono who gave me this wonderful opportunity to pursue my PhD to this level. I would like to express my sincere appreciations to my co-supervisor Prof. Dr Rafiq for his guidance in my research.

During the course of this PhD project, I had the chance to collaborate with some research groups and collaborative researchers. I would like to thank Prof. Seeram Ramakrishna and Dr. Molamma P. Prabhakaran who gave me the opportunity to pursue my research internship and to carry out my experiments at Centre for Nanofibers and Nanotechnology in National University of Singapore (NUS) for a period of one year. I have been lucky to have had the opportunity to work in the faculty of Bioscience and Medical Engineering in University Technology Malaysia during these four years, and for this I would like to thank to UTM for providing me facilities and equipment. I would like to extend special thanks to Syazwani, Salasiah, Fahimeh, and Nabila for their contributions to my research work, and my sincere thanks to my colleagues in Bio-inspired Medical Devices Lab, Syamsiah, Lam and others for their sharing knowledge and assistance in lab-works.

Others have also helped me in specific ways. Many thanks to all technicians and operators for their cooperation in operating equipment, especially, Norhidayu

who helped me with XPS measurements. I appreciate Ms. Mei Hong Ooi and Dr. Fei-Tieng Lim for helps on SEM measurements and Confocal Laser Scanning Microscopy at Hi-Tech Instruments.

I owe my gratitude to my dear friends, Rokhsareh, Mojib, Fatemeh, Sara and Radha for their constant encouragement. I am pleased to thank Mahdi for his help in formatting of my thesis document and also I am thankful to Aisyah to translate the abstract to Bahasa Malay. Lastly, I would like acknowledge security personnel of faculty of bioscience and medical engineering for their kind patience and cooperation, especially during last year of my PhD studies.

I have been blessed with wonderful family who stuck by me through both good and bad times. I give my deepest thanks to my beloved husband (Mr. Mohammadreza) for his constructive feedback and advice on my research work and his amazing love and support as the source of inspiration.

Finally, I would like to acknowledge all financial support from Universiti Teknologi Malaysia (UTM).

ABSTRACT

Micro/Nanofluidics technology is a new research area focused on analyzing and controlling flow of fluids and bio-particles at nanometer and micrometer scales. In an attempt to achieve low cost fabrication and operation of microfluidic devices, the use of cotton fabric was proposed as a new platform for developing low-cost microfluidic devices. This thesis presents a novel wicking fluidic study through the hierarchical structures of textiles by multi-stage analysis of fluid flow at different structural scales, from the macro- (the three dimensional network structure of the cotton fabrics), via the micro- (the tiny segment of the textile structure, twisted multi fibers in a yarn) to the nanoscale (single fiber). The wicking flow within the cotton fabric structure and kapok fiber (as a hollow fiber and a simple model for the wicking flow) was experimentally analyzed using quantitative fluorescence microscopy data from the motion of fluorescent beads. Thereafter, in order to formulate the wicking flow through the hierarchical structure of the fibers network of the cotton fabrics and to predict how the wicking flow depends on the textile structure and basic material properties, experimental analyses based on fluorescent beads tracing with fluorescent and confocal microscopy as well as analytical analyses were carried out. The results of this study formed the foundation of new theories and novel ideas for interfacing microfluidics and nanofluidics. Additionally, the analyses prove that the wicking and the capillary action play important roles in selective mass transport in the textile structures. This phenomenon is potentially useful for biological and chemical detection in biosensors devices. The research targets application in novel passive size-based mechanical cell sorting using cotton fabric chip and fiber based enzyme-linked immunosorbent assay (ELISA).

ABSTRAK

Teknologi bendalir-mikro/nano adalah era baru penyelidikan yang fokus kepada penganalisan dan pengawalan aliran cecair serta partikel-bio yang berskala nanometer dan mikrometer. Dalam usaha untuk mencapai kos fabrikasi dan operasi alat mikrobendalir yang rendah, penggunaan fabrik kapas telah dicadangkan sebagai satu platform baru. Tesis ini membincangkan satu kajian original berkenaan resapan bendalir melalui struktur hierarki kain menggunakan analisis pelbagai peringkat aliran bendalir untuk perbezaan skala struktur daripada makro (tiga dimensi rangkaian struktur fabrik kapas), mikro (bahagian kecil struktur tekstil, pelbagai benang yang dipintal) kepada nano (serat tunggal). Penyerapan bendalir dalam struktur fabrik kapas dan serat kapok (sebagai satu serat berlubang dan model ringkas untuk kadar penyerapan) telah dianalisis secara eksperimen menggunakan data kuantitatif pendarfluor mikroskop daripada pergerakan manik pendarfluor. Oleh itu, untuk memformulasi kadar penyerapan melalui struktur hierarki rangkaian serat fabrik kapas dan meramalkan bagaimana kadar penyerapan bergantung kepada struktur tekstil dan sifat asas bahan, analisis secara eksperimen berasaskan manik pendarfluor dan mikroskop sefokus serta analisis secara analitikal telah dilakukan. Keputusan kajian telah menghasilkan teori asas baru dan idea original untuk interaksi antara mikrobendalir dengan nanobendalir. Selain itu, beberapa analisis membuktikan bahawa serapan dan tindakan kapilari memainkan peranan penting dalam pemilihan dalam struktur tekstil. Fenomene ini amat berguna untuk pengesanan biologi dan bahan kimia di dalam alat biopenderia. Aplikasi sasaran kajian ini ialah pengisihan sel mekanikal berasaskan saiz pasif menggunakan cip fabrik kapas dan serat berasaskan asai imunoserap terangkai ensim (ELISA).

TABLE OF CONTENTS

CHAPTER	TITLE	PAGE
	DECLARATION	ii
	DEDICATION	iii
	ACKNOWLEDGEMENTS	iv
	ABSTRACT	vi
	ABSTRAK	vii
	TABLE OF CONTENTS	viii
	LIST OF TABLES	xv
	LIST OF FIGURES	xvi
	LIST OF SYMBOLS	xxvi
1	INTRODUCTION	1
	1.1 Introduction	1
	1.2 Background of the study	2
	1.3 Problem statement	5
	1.4 Objectives of the study	5
	1.5 Scopes	6
	1.6 Thesis outline	7
2	LITRATURE REVIEW	9
	2.1 Introduction	9
	2.2 Biomicrofluidic devices based on threads and fabrics	9
	2.3 Physics of microscale fluid mechanics in microfluidic systems	10
	2.3.1 Laminar flow in microfluidics systems	11
	2.3.2 Diffusion	12

2.3.3	Fluidic resistivity	13
2.3.4	Surface-area-to-volume ratio	13
2.3.5	Surface tensions, hydrophilicity, hydrophobicity and capillary effects	14
2.4	Properties of cotton fiber	16
2.4.1	Composition of cotton fiber	16
2.4.2	Chemistry of cotton cellulose	17
2.4.3	Structure of cotton from fiber to fabric	19
2.5	Structure and chemical composition of kapok fiber as a natural cellulose hollow fiber	21
2.6	Capillary and wicking flow properties in multifilament of fibers, thread and fabric	23
2.6.1	Mathematical model	26
2.6.2	Capillary flow calculation	27
2.7	Conclusion	28
3	WICKING FLOW ANALYSIS THROUGH THE HIERARCHICAL STRUCTURE OF NATURAL CELLULOSE FIBERS	29
3.1	Introduction	29
3.2	Material and Methods	32
3.2.1	Chemical treatment of kapok and cotton fibers	32
3.2.1.1	Raw material	32
3.2.1.2	Treatment of a kapok fiber with sodium hydroxide, (NaOH) followed by sodium chlorite (NaClO ₂)	32
3.2.2	Scouring treatment of a cotton fiber, thread and fabric with soda ash, Na ₂ CO ₃	33
3.2.3	Morphological study of the hierarchical structure of textile	33
3.2.3.1	Scanning electron microscopy (SEM)	33
3.2.3.2	Atomic force microscopy (AFM)	34
3.2.4	Surface chemical characterization of a kapok and a cotton fiber after and before treatment	34

3.2.4.1	X-ray spectroscopy (EDS)	34
3.2.4.2	FTIR Fourier Transform infrared Raman-spectroscopy (FTIR)	35
3.2.4.3	X-ray Photoelectron Spectroscopy (XPS)	35
3.2.4.4	Thermo gravimetric analysis (TGA)	35
3.2.5	Wicking and wetting analysis	36
3.2.5.1	Wettability measurement using contact angle measurement	36
3.2.5.2	Experimental study by Confocal Laser Scanning Microscopy (CLSM)	37
3.2.5.3	Quantitative analysis of wicking dynamics through the fibrous structure of natural cellulose fibers	37
3.3	Results and discussions	39
3.3.1	Physical characteristics of fibers after chemical modification	39
3.3.1.1	Surface morphology characterization by SEM results	40
3.3.2	Energy dispersive spectroscopy analysis	45
3.3.3	Atomic Force Microscopy (AFM) to analysis surface roughness	46
3.3.4	Characterization of surface chemical composition by FTIR result	48
3.3.5	Characterization of surface chemical composition of treated and untreated kapok fiber by X-ray Photoelectron Spectroscopy (XPS)	50
3.3.6	Thermo gravimetric analysis (TGA)	55
3.4	Wetting properties analysis of natural cellulose fibers	56
3.5	Capillary and wicking flow through single natural cellulose fiber	57
3.5.1	Surface wicking analysis on the surface of fiber	57
3.5.2	Translumen wicking observation	60

3.5.3	Vertical interstitial wicking	62
3.5.4	Verification of analytical wicking models based on experiments:	62
3.6	Conclusion	63
4	A PASSIVE SIZE-BASED MECHANICAL CELL SORTING USING A COTTON FABRIC CHIP	65
4.1	Introduction	65
4.2	Material and Methods	67
4.2.1	Material	67
4.2.2	Scouring treatment of cotton fabric	67
4.2.3	Scanning Electron Microscopy (SEM)	68
4.2.4	Surface roughness measurement	68
4.2.5	Surface chemical characterization of cotton fabric	68
4.2.6	Pore size distribution and capillary flow investigation	68
4.2.7	Wicking investigation along warpwise and weftwise on the cotton fabric	69
4.2.8	Fabrication of a fabric-based cell sorting device with wax patterning:	69
4.2.9	Preparation of suspend fluorescent polystyrene beads in water	71
4.2.10	Culturing and fluorescent staining of hybridoma, fibroblast and cancerous fibroblast cells	72
4.2.11	Investigation of wickability and sortability of beads/cells	73
4.2.12	Statistical study on wickability and sortability	74
4.3	Results and discussions	74
4.3.1	Surface structure characterization by SEM	74
4.3.2	3-D surface measurement	76
4.3.3	Surface chemical characterization	77

4.3.4	Pore size distribution and capillary flow characterization	79
4.3.5	Wicking flow analysis along warp and weft direction on cotton fabric	81
4.3.6	Cells/Beads wickability along the hydrophilic channels of a cotton fabric chip	88
4.3.7	Effect of hydrophilic channel dimension on cells/beads wicking:	89
4.3.8	Cells/Beads sortability along the hydrophilic channels of cotton fabric chip	94
4.4	Conclusion	97
5	THREAD BASED CELLS SORTING MICROFLUIDICS DEVICE	99
5.1	Introduction	99
5.2	Experimental method	100
5.2.1	Fabrication of thread-based cell sorting device	100
5.2.2	Blood processing	102
5.3	Results and Discussion	102
5.3.1	Wicking analysis on a thread	102
5.3.2	The sortability of cells and beads with different sizes through the thread-based microfluidic device:	104
5.3.2.1	Confocal microscopy analysis on the sortability of fluorescent beads with different sizes through the thread-based devices	105
5.3.2.2	Scanning electron microscopy analysis on blood cells sorting through the thread-based microfluidic device	107
5.4	Conclusion	110
6	FIBER-BASED CRP-ELISA	111
6.1	Introduction	111

6.2	Materials and Methods	114
6.2.1	Materials	114
6.2.2	Electrospinning of nanofibers	114
6.2.3	Characterization of nanofibrous scaffolds and fibers in cotton swabs	115
6.2.4	Crosslinking of fibers	115
6.2.5	Immobilization of antibody on electrospun nanofibers and cotton swab fibers	116
6.2.6	Binding ability of nanofibrous membrane with anti-CRP antibody	116
6.2.7	Development of optical CRP-ELISA on PLLA nanofibrous membrane	117
6.2.8	Development of colorimetric CRP-ELISA on CA nanofibrous mat and cotton swabs	119
6.2.9	Statistical and image analysis	120
6.3	Results and Discussion	121
6.3.1	Characterization of fibers	121
6.3.1.1	Characterization by Scanning Electron Microscopy (SEM)	121
6.3.1.2	Wettability characterization of nanofibers and micro cotton fibers	123
6.3.1.3	Chemical characterizations of fiber surfaces	123
6.3.1.4	Binding of primary antibody to electrospun nanofibrous membrane	124
6.3.2	Optimization of efficiency parameters on the performance of fiber based CRP-ELISA	127
6.3.3	Analytical performance of fiber based CRP immunoassays with optimized parameters	130
6.3.4	Calculation of limit of detection	134
6.3.5	Stability of fiber based CRP immunoassays	134
6.4	Conclusion	136

7	CONCLUSION AND OUTLOOK	138
	7.1 Conclusion	138
	7.2 Future work	139
	REFERENCES	141
	Appendices A-B	157-174

LIST OF TABLES

TABLE NO.	TITLE	PAGE
2.1	Elements of cotton fiber	16
2.2	Components of cotton fiber [55]	18
2.3	Cotton Fiber Structure [55]	20
2.4	Components of the kapok fiber [62]	23
4.1	Measured roughness and mean scale heights of treated and untreated cotton fabric by Alicona InfiniteFocus 3D True Colour Optical Profiler	77
4.2	Measured and calculated effecting parameters on macrocapillary and microcapillary rise through cotton fabric structures	85
6.1	Characterization of electrospun nanofibers, micro cotton fibers of cotton swabs and conventional ELISA plate	122
6.2	Comparison of time period of CRP-ELISA performed on nanofibers and microfibers compared to conventional method	128
6.3	Linear and logistical model parameters of conventional ELISA and fiber based ELISA	136
B.1	Preparation of standard maltose curve by following reaction mixture	164
B.2	Conventional alpha-amylase assay	164
B.3	Normal range of α -amylase in saliva based on Takai, et al. [174]	172

LIST OF FIGURES

FIGURE NO.	TITLE	PAGE
1.1	Flowchart representation of the thesis structure	8
2.1	Schematic of a water droplet on the hydrophobic and hydrophilic surfaces.	15
2.2	(a) Cellulose formula (C ₆ H ₁₀ O ₅) _n , (b) The hydrogen bonds between glucose strands in triple strand of cellulose. Reprinted with permission from [59].	18
2.3	(a) Microscopic view of cotton fiber; (b) Structure of cotton fiber. (Primary, secondary walls and lumen of cotton fiber). (c) Cotton fiber's cross-sectional shapes (1. wax layer. 2. primary wall. 3. secondary wall. 4. tertiary wall. 5. lumen). Reprinted with permission from [59]	19
2.4	(a) <i>Ceiba pentandra</i> tree, (b) kapok fruit and (c) kapok fiber.	22
2.5	SEM images of kapok fibers, (a) longitudinal view, (b) cross section. Reprinted with permission [66].	22
2.6	Thread position in fabric considering as inclined tube geometry. Represented with permission [80]	25
2.7	Plain weave in which the weft and warp threads intertwine alternately to produce a checkerboard effect	25
2.8	Woven fabric with and without the cross weft threads. Reprinted with permission [80].	26
3.1	Schematic of surface modification of natural cellulose fiber	31

3.2	Schematic of three different wicking flows through the single fiber structure; translumen, nanopore-translumen and surface wicking	39
3.3	SEM images from (a, b) untreated and (c, d) Na ₂ CO ₃ treated natural cotton fiber under different magnifications (1000X – 10000X). The images show the scouring treatment removes the waxy layer from the surface and underlys spiral microcellulose fiber.	41
3.4	SEM morphology images of raw kapok fiber under different magnifications	42
3.5	SEM images from cross section of single untreated kapok fiber with 20μm diameter	42
3.6	SEM morphology of treated kapok fiber with NaOH aqueous 5% under various magnifications; (a) 1000X, (b) 3500X, (c) 5000X and (d) 20000X. The images show that microfibrils and some pores appear on the surface of kapok fiber after treatment	43
3.7	SEM morphology of treated kapok fiber with NaOH aqueous 20% under different magnifications; (a) 1000X, (b) 3500X and (c) 20000X. The images presents that the structure of fiber is damaged due to scouring treatment with high concentration of NaOH solution.	44
3.8	Schematic of lignin and hemicellolus extraction from natural fibers after chemical treatment	44
3.9	SEM morphology of treated kapok fiber with NaOH aqueous 3%, sodium chlorite (NaClO ₂) aqueous 10% and HCl.	45
3.10	EDS spectrum of (a) natural kapok fiber, (b) alkali-treated kapok fiber with NaOH 15 % and (c) treated kapok fiber with NaClO ₂ , NaOH, HCl. The graphs and tables describe that the percentage of oxygen- O increased after treatment, whereas, the percentage of carbon-C decreased due to extracted lignin and wax.	46

- 3.11 AFM topographies of (a) natural cotton fiber, (b) treated cotton fiber with Na_2CO_3 , (c) raw kapok fiber, (d) scouring treated kapok fiber with NaOH and (e) scouring and bleaching treated kapok fiber with NaOH and NaClO_2 . The images illustrate that the roughness (Ra) of surface fiber increases after treatment. 48
- 3.12 FTIR spectra of treated and untreated kapok fibers. 49
- 3.13 FTIR spectra of natural cotton fibers and scouring treated fiber with Na_2CO_3 50
- 3.14 XPS survey of natural kapok fiber. (a) survey scan; (b) XPS O1s spectrum: the experimental data (black curve) decomposed to C-OH (blue curve) and C=O (red curve) component ; and (c) XPS C1s spectra: the experimental data (black curve) decomposed to C-CH (blue curve), C-O (red curve), C=O (red curve) and ester (orange curve) component. 52
- 3.15 XPS survey of scouring treated kapok fiber. (a) survey scan; (b) XPS O1s spectrum: the experimental data (black curve) decomposed to C-OH (blue curve) and C=O (red curve) component ; and (c) XPS C1s spectra: the experimental data (black curve) decomposed to C-CH (blue curve), C-O (red curve), C=O (red curve) and ester (orange curve) component. 53
- 3.16 XPS survey (a) scan and (b, c) spectra XPS survey of bleaching and scouring treated kapok fiber. (a) survey scan; (b) XPS O1s spectrum: the experimental data (black curve) decomposed to C-OH (blue curve) and C=O (red curve) component ; and (c) XPS C1s spectra: the experimental data (black curve) decomposed to C-CH (blue curve), C-O (red curve), C=O (red curve) and ester (orange curve) component. 54
- 3.17 TGA signals of (a) natural kapok fiber, (b) scoured, and (c) scoured and bleached kapok fiber. The results for the analyzed kapok material verified that two steps

	of degradation for fibers at 220-270 °C and 320-360 °C are due to the decomposition of hemicellulose and lignin.	55
3.18	Water contact angle on a bulk of (a) treated (scouring and bleaching) and (b) untreated kapok fibers (c) Water diffusion through the kapok fiber wall of treated kapok fibers after $t=0.16$ s.	56
3.19	Surface wicking of beads with size of $1\mu\text{m}$ along the micro-grooves of (a) cotton fiber surface and (b) kapok fiber surface.	58
3.20	Surface wicking flow based on capillary action through the micro-grooves of the surface	59
3.21	Translumen wicking of beads with size of 200 nm through the lumen of kapok fiber in four interval times, $t_1 = 0.2$ s, $t_2 = 0.4$ s, $t_3 = 0.6$ s, $t_4 = 0.8$ s.	60
3.22	Bubbles and droplet formation inside of the lumen of the kapok fiber	61
3.23	Water absorption to the lumen through micro and nano pores of fiber surface	62
3.24	Experimental results from surface wicking and capillary translumen wicking test.	63
3.25	Analytical analysis of surface wicking and translumen capillary wicking in respect to time.	63
4.1	A schematic of the size-based mechanical cell/beads sorting on fabric chip	66
4.2	Schematic illustration fabric chip fabrication process with simple wax patterning techniques; a) wax impregnated paper, b) creating a pattern of hydrophilic channel, c) transfer of wax from a paper to the cotton fabric by heat treatment, d) creating a hydrophilic channel on the cotton fabric chip.	70
4.3	Designs of simple hydrophilic patterns with one inlet and outlet on fabric based cell-sorting chip	71

- 4.4 SEM secondary electron SEM images (SEI) of (a, b) untreated cotton fabric and (c, d) treated cotton fabric 75
- 4.5 SEM image at (a) interfacing between wax impregnated and non-waxy cotton fabric region and zoom-in images on (b) non-waxy and (c) wax impregnated fibers. 76
- 4.6 3D surface profile of (a) untreated and (b) treated cotton fabric 77
- 4.7 Atomic carbon and oxygen percentage on hydrophobic wax barrier (a and c) and hydrophilic cotton channel (b and d). The first two groups of bars (a and b) present the percentage values for untreated cotton fabric; the last two groups of bars (c and d) are for treated cotton. The blue bars show the composition of carbon and the red bars are for oxygen. 78
- 4.8 SEM and the corresponding EDS spectra from (a) waxed and (b) un-waxed region of untreated cotton fabric in comparison with (c) waxed and (d) un-waxed region of treated cotton fabric by Na_2CO_3 79
- 4.9 Wet, dry and half dry curves for woven cotton fabric. The red curve presents the nitrogen gas flow rate (L/min) through the dry sample with dry pores. The green line is called half-dry curve which is obtained by dividing the dry curve's values by 2. The blue line is the gas flow rate through wet pores. The wetted pores become dry after some curtain pressures, whereby, the gas flow rate reaches to the one in dry sample. The pore sizes are then calculated on the basis of imposed pressure and nitrogen flow rate at the intersecting point. 80
- 4.10 Schematic of Microcapillary in a thread [118]. It is assumed that the R_μ is an effective radius for the space between the fibers in a thread; thus, its value depends

	on the number of fibers in a yarn, tortuosity of yarn and diameters of fibers.	82
4.11	Schematic of macrocapillary between yarns [118]. It is assumed that the capillary between the yarns regarded as capillary between two parallel plates. The length of plates (L) is the unit cell of plain weave (top schematic). “L” is “a” if it is warp way capillary or “L” is “b” if it is weft way capillary.	83
4.12	Experimental setup for (a) vertical and (b) horizontal wicking	86
4.13	Experimental results from horizontal and vertical wicking test. The wicking length is recorded every 30 seconds.	87
4.15	Length optimization of hydrophilic channel on cotton fabric due to wickability of beads with 10 μm size.	89
4.16	Width optimization of hydrophilic channel on cotton fabric due to wickability of beads with 10 μm size	90
4.17	Dynamic data analysis of numbers of 10 μm beads versus time at 7 different position of hydrophilic channel	91
4.18	Stationary data analysis from beads and cells distribution through the hydrophilic channel.	91
4.19	Dynamic data analysis from wickability of three different size of polystyrene fluospheres (a) 4 μm , (b) 10 μm and (c) 15 μm	93
4.20	The beads mixture sorting through the fabricated cotton fabric chip.	94
4.21	Confocal images from inlet, middle and outlet of hydrophilic channel. Red dots are 10 μm beads and small green dots are 4 μm beads	95
4.22	Confocal images from inlet, middle and outlet of hydrophilic channel. Red dots are 15 μm beads and small green dots are 4 μm beads	95

4.23	Size based-distribution of the beads fractions in inlet, middle and outlet for two different mixtures including a mixture of 4 and 10 μm beads and a mixture of 4 and 15 μm beads.	96
4.24	SEM images from inlet, middle and outlet of hydrophilic channel to find beads sorting from the mixture of 4 and 10 μm beads solution	96
4.25	SEM images from inlet, middle and outlet of hydrophilic channel to find beads sorting from the mixture of 4 and 15 μm beads solution	97
5.1	Schematic design of thread-based cell sorting devices	101
5.2	The wicking test set-up	103
5.3	Wicking rate analysis for threads with different TPIs	104
5.4	Three focused position on thread for wickability study	105
5.5	Confocal images from zone-1 (near inlet before first knot) where 15 μm beads were trapped at the area near to the inlet(red colors)	105
5.6	Confocal images from zone-2 (at the second zone after the first knot) where no red color beads (15 μm) were observed.	106
5.7	Confocal images from zone-3 (at the third zone after the second knot) where no red color beads (15 μm) were observed.	106
5.8	Size-based distribution of the bead fractions in three zones.	107
5.9	Blood cells sorting through the fabricated thread-based device	108
5.10	SEM images from first position near the inlet where the WBCs are trapped	109
5.11	SEM images from second zone where the RBCs are trapped a) near the first knot, b) in the middle zone between two knots	109

5.12	(a) SEM images from third zone a) the few RBCs are trapped at the second knot, b) there is no RBCs after second knot.	110
6.1	Schematic on the development of electrospun fiber based sandwich CRP-ELISA: 1) electrospinning of nanofibers and collecting on 15 mm coverslip, 2) Placing 15mm coverslip contained nanofiber mat within the wells of a 24-well plate, 3) Entrapment and coupling with EDC/NHS, 4) Capturing anti-CRP immobilized on nanofibers mat, 5) Blocking the surface of nanofibers with BSA, 6) Incubating nanofibers with samples and standards with different level of CRP, 7) Incubating nanofibers with HRP-labeled signal antibodies	118
6.2	Concept of cotton swabs based CRP-ELISA and schematic on its development: 1) Placing cotton swabs within microtube of a 24-microtube plate, 2) Entrapment and coupling with EDC/NHS, 3) Capturing anti-CRP immobilized on nanofibers mat, 4) Blocking the surface of nanofibers with BSA, 5) Incubating nanofibers with samples and standards with different level of CRP, 6) Incubating nanofibers with HRP-labeled signal antibodies.	120
6.3	Scanning electron microscopy (SEM) images (A-C) and histogram showing the fiber size distribution (D-F) of electrospun PLLA (A, D), electrospun CA nanofibers (B, E) and cotton fibers in cotton swabs (C, F)	122
6.4	Contact angle images of (a) PLLA, (b) CA electrospun nanofibers and (c) cotton fibers in cotton buds	123
6.5	FTIR spectrum of PLLA, CA nanofibers and cotton swabs immobilization	124
6.6	UV-Vis spectra from leached BSA on (A) PLLA nanofibers, (B) CA nanofibers, (C) Cotton swabs,	

	before antibody immobilization and after antibody immobilization (D) Standard calibration curve of standards that are used to determine the concentration of BSA in leached solutions. (E) Calculated amounts of BSA adsorbed on PLLA, CA and cotton swabs	126
6.7	Optimization of incubation time for (A, B) antibody immobilization, (C, D) samples and (E, F) signal amplification of CRP signal in all fiber based CRP-ELISA	129
6.8	Standard calibration curve for (A) conventional and (B) PLLA nanofibers-based CRP-ELISA as functions of mean absorbance (OD) vs. CRP concentration were fitted with the 4-parameters logistic regression (4-PLR) curve.	131
6.9	The optical intensity (a.u) as function of CRP concentrations for CA nanofibers were plotted in 4-PLR calibration curves	132
6.10	4-PLR calibration curves for cotton swabs CRP-ELISA	133
6.11	Stability of fiber-based CRP-ELISAs examined by plotting the 4-PLR calibration curves and linear fittings for (A) PLLA nanofibers, (B) CA nanofibers and (C) cotton swabs CRP-ELISA after two weeks storage at 4 °C.	135
B.1	Cotton swab-based α -amylase assay procedures	166
B.2	Wicking properties of twisted cotton swab with different TPI 4, 7 and 12.	167
B.3	Colorimetric calibration standard curve for serial concentrations of maltose on (a) cotton swab and (b) 96 wells plate	169
B.4	Converting color image to grayscale through image intensity processing by ImageJ	170
B.5	Plotting calibration standard curve for serial concentrations of maltose on (A) conventional assay based on Bernfeld and (B) cotton-swab-based device.	170

- B.6 Plotting calibration standard curve for serial concentrations of alpha amylase on (A) conventional assay based on Bernfeld and (B) cotton-swab-based alpha-amylase assay 172
- B.7 The salivary α -amylase level in rest and stress condition. Represented with permission from [175]. 173

LIST OF SYMBOLS

A	-	Area
ACS	-	Acute coronary syndromes
AFM	-	Atomic Force Microscopy
AMI	-	Acute myocardial infarction
ATR	-	Attenuated total reflectance
A_{welf}	-	Cross-sectional area of pore exposed to the welf way
A_{wrap}	-	Cross-sectional area of pore exposed to the wrap way
BSA	-	Bovine serum albumin
c_1, c_2	-	Wrap and welf crimp
CA	-	Cellulose acetate
CLSM	-	Confocal laser scanning microscopy
CRP	-	C-reactive protein
CSA	-	Camphorsulfonic acid
CVD	-	Cardiovascular disease
D	-	Diffusion coefficient
d	-	Diameter
DNS	-	Dinitrosalicylic acid

E	-	Interfacial energy
ECG	-	Electrocardiogram
EDA	-	Energy-dissipative electron spectroscopy
ELISA	-	Enzyme-linked immunosorbent assay
FESEM	-	Field-Emission Scanning Electron Microscopy
FTIR	-	Fourier transformation infrared roman spectroscopy
g	-	Gravity acceleration
HBSS	-	Hank's balanced salt solution
HF	-	Heart failure
h_{fab}	-	Wicking height in fabric
HFP	-	1,1,1,3,3,3-hexafluoro-2-propanol
J	-	Diffusion flux
K_n	-	Knudsen diffusion
L	-	Length
l_2	-	Modular length in transverse direction
LOD	-	Limit of detection
MI	-	Myocardial infarction
n_2	-	Number of weft threads
O.D.	-	Optical Density
p	-	Pressure
p_1, p_2	-	Wrap and welf spacing

<i>PAD</i>	-	Paper-based analytical device
PANI	-	Polyaniline
PBS	-	Phosphate Buffered Saline Solutions
PDMS	-	Polydimethylsiloxane
PLLA	-	polylactic acid
PMMA	-	Poly(methyl methacrylate)
POC	-	Point of care
PS	-	Polystyrene
<i>Q</i>	-	Volume fluid flow
<i>R</i>	-	Fluid resistance
<i>Ra</i>		Roughness
RBC	-	Red blood cell
<i>Re</i>	-	Reynolds
RMS	-	Root mean square
<i>R_μ</i>	-	Capillary radius
SAA	-	Salivary alpha amylase
SD	-	Standard deviation
SEM	-	Scanning Electron Microscopy
SWNT	-	Single-well carbon nano-tube
<i>t</i>	-	Time
<i>TAD</i>	-	Thread-based analytical device

TE	-	Thromboembolic
TGA	-	Thermal gravimetric analysis
TMB	-	Tetramethylbenzidine
TPI	-	Twisting per inch
u	-	Velocity
UV	-	Ultraviolet
WBC	-	White blood cell
WGA	-	White germ agglutinin
x	-	Particle travel distance
XPS	-	X-Ray Photoelectron Spectroscopy

LIST OF APPENDICES

APPENDIX	TITLE	PAGE
A	List of publications	157
B	Low cost cotton swab-based salivary alpha-amylase assay for stress level detection	159

CHAPTER 1

INTRODUCTION

1.1 Introduction

Recently, microfluidics technologists have developed different devices for the fast manipulation and characterization of fluid samples for biological and the chemical analyses. Microfluidic devices commonly consist of microscale fluidic channel with typical length of 1-100 μm . High throughput analysis, small sample volume, shortened analysis time, enabling new functionalities by integrating new micro components and application of novel physics phenomena; all these are reported benefits for microfluidics devices. In typical bio-diagnostic microfluidic systems, multiple different fluidic elements are connected into circuits to detect a specific analyte in a sample fluid.

Nanofluidics refers to the study of fluidics in nanochannels in the length scale of 1-100 nm. The unique physics phenomena behind the working of nanofluidics devices can be revealed by studying fluid flow in such devices. Since the channel sizes in nanofluidics are closed to biomolecule size, most of the time nanofluidics have been applied to carry out separation, to count or to characterize individual biomolecules such as protein or DNA molecules.

Many different fabrication techniques are reported to develop microfluidics, nanofluidics and interfacing them together. However, all of these methods require considerable cost and specialized equipment to reduce the high development cost for the fabrication and operation of modern microfluidic and nanofluidic devices that are

made up of materials such as, silicon [1], glass [2], and polymers i.e. PMMA [3], SU-8 [4] and PDMS [5, 6]. Microfluidic systems that are intended to be low cost and portable for home-use diagnostic applications have been proposed by many researchers. These microfluidic systems are made from hydrophilic materials such as paper [7, 8], threads [9, 10] and cloth like silk [11] and cotton [12]. Since capillary force wicks and drives liquids in their hydrophilic microchannels, no pumping system and advanced control system is necessary in such microfluidic systems.

Capillary effect is also known as wicking and has been widely used as a pumping force in microfluidic systems in recent years. Capillary pumping is surface-directed and has no external power input. It exhibits a small pressure drop in the micro channel. Hydrophilic surface is essential for capillary pumping. Relevant capillary effect issues in microfluidic chips have been studied in terms of the theory, channel geometry, patterned structure and applications [13-17].

1.2 Background of the study

Intensive demand to have sensitive, simple and portable biodiagnostic devices especially in developing countries has received much attention. Such devices exploit low-cost, disposable and hydrophilic materials (such as paper, thread and fabric) to create a hydrophilic pattern to form a microfluidics device platform for medical diagnostics test.

Microfluidics paper-based analytical devices (μ PADs) have been developed for point of care diagnostics and environmental monitoring at resource-poor regions. The concept of paper based microfluidics was first proposed by the Whiteside research group at Harvard University [7]. Most of the μ PADs have been fabricated by patterning hydrophobic barriers on Whatman filter paper. Wax [18, 19], polystyrene [20], polydimethylsiloxane [5], alkyl ketene dimer [21] and fluorochemicals [22] have been used as the materials for patterning hydrophobic barriers on the paper. Different patterning methods have also been applied for patterning the hydrophilic channels on paper such as photolithography [7], printing

[18] plasma [23], laser [24] and chemical etching method [25]. Due to simplicity and compatibility with aqueous solutions, the Whiteside's wax printing has become one of the popular techniques for μ PADs fabrication. The limitations of paper based microfluidic devices mostly are related to the material properties of paper. Some of the limitations are as follows:

- Low wetting strength of paper [26].
- Low efficiency of sample delivery due to sample retention and evaporation through the hydrophilic channels on the surface of paper [27].
- Low strength of the patterned hydrophobic barrier on paper [27].

Thread [9, 10] and fabric [11, 12] have been applied as low-cost platforms for developing inexpensive microfluidic devices. The gaps between the fibers on the thread and between the yarns in textiles are considered as capillary channels to move liquid without external forces or pumping effect. This capillary force and driven liquid in the hydrophilic multi-filaments microchannels define the wicking properties of these structures. Researchers proved that coated waxes on the natural fibers decrease or even stop fluid wicking within the threads of cotton fabric [28]. To overcome the aforementioned problem, various surface modification methods were reported to remove natural wax from the fiber's surface to improve their wettability of the fibers and consequently also the wicking capillary action occurred in the porous fiber structure of threads and cotton fabric [12].

Several microfluidic thread-based analytical devices (μ TADs) have been reported as a colorimetric assay device to detect glucose and protein in urine or blood [10, 29]. Thread was also used for blood typing [30]. The advantages of thread compared to paper are its flexibility and wet strength. The fabrication of thread-based microfluidic devices is simpler and relatively low cost, because it requires only sewing needles or household sewing machines.

Designing and developing microfluidics devices based on the multiplex and multiple-dimensional thread is relatively difficult, since one-dimension is assumed for thread. On the other hand, a publication by our research group reported an innovative two- and three-dimensional cotton fabric-based microfluidic devices which was developed based on the two-dimensional fabric [12]. We have proved their potential as unconventional assay for glucose, nitrate and protein detection, and as quick colorimetric enzyme-linked immunosorbent assay (ELISA) to determine human chorionic gonadotropin [31]. In another recent paper, cotton fabric was used for developing a microfluidic device to electrochemically detect lactate level in saliva [32]. Several advantages of thread and cotton fabric versus papers to develop microfluidic systems are listed below;

- High flexibility due to great tensile strength; wicking and reaction still happen despite bending, twisting, stretching and compression [28].
- Long term mechanical durability; despite the platform being bent, stretched, comprised or twisted [33].
- Long term continuous flexible sampling; it can endure liquid wicking without damaging the structure, under various mechanical disturbances [32].
- Additional porous structure due to the wide variety of pores: higher surface area to volume ratio which guarantee higher sensitivity of thread and fabric-based assays [31].

Both thread and fabric have a wide-ranging diversity of pores and gaps such as nanopores and gaps between the cellulose microfibrils in a single fiber, microscale interfiber gaps and inertial void spaces between the twisting and weaving fibers in the thread and the yarns in the cotton fabric. Therefore, the wicking flow characterization inside this hierarchical structure is difficult to carry out and requires further study. In this study, capillary and wicking flow through the complex and porous structure of natural fibers and hierarchical structures of cotton fabric are investigated. The aim of this study is to develop inexpensive and simple

micro/nanofluidic devices from the multi filaments of natural fibers including fibers, thread and fabric for biological and chemical applications.

1.3 Problem statement

In this study, we aim to characterize and develop models of liquid wicking on cotton fibers, thread and fabrics to meet emerging technical and performance needs in micro/nanofluidics applications, e.g. biomedical devices and chemical/biological devices. In this manner, understanding how liquids wet, permeate and flow in multiscale porous fibrous structures is important.

Characterizing the physical and mechanical properties of the complicated and hierarchical structures of cotton fabric is no a small task. Wicking flow and Fluid interactions through these structures of cotton fabric, especially considering their pore size diversity, further adds the complexity. Wetting and wicking of fluids through fibrous structures is dynamic and stochastic, often involving changing physical nature due to surface adsorption, fiber shifting and fiber swelling. Characterizations of fluid wicking phenomena in the fibrous structures of fibers to fabric is extremely required to precise by control fluid flow in microfluidics system which are fabricated from fibers, thread or fabric.

1.4 Objectives of the study

1. Study on the morphology and the hierarchical structure of the textile, from fiber to fabric, single fiber (cotton and kapok fiber), cotton thread and fabric.
2. Experimental measurements of the wetting properties and the wicking rate of single fiber to fabrics and correlating them to analytical and mathematical modelling.

3. Study on fluidic wicking through the hierarchical fibrous structure of cotton fabric by multi-stage analysis of the fluid flow at different scales from the micro- (through three-dimensional network structure of the cotton fabric, tiny segment of textile structure or twisted multifibers in thread) to the nanoscale (in a single fiber).
4. Designing and developing cotton thread and fabric-based microfluidics devices for a passive size-based mechanical cell sorting by characterization the wickability and sortability of multiple sizes of beads and cells through the fibrous structure of the devices.
5. To design a fiber-based assay and an enzyme linked immunosorbent assay (ELISA) with high sensitivity by utilizing the high surface area to volume ratio property.

1.5 Scopes

1. Chemical modification is conducted to modify the surface chemical composition and surface morphology of the fiber.
2. Prior to the further studies of multiscale fluid flow, the hierarchical structures and morphology of the textile should be carried out based on the microscopy studies.
3. In the next stage of the study, the wicking movement of fluid along a single fiber, spun fibers and thread with different twistings per inch (TPI) and a strip of cotton fabric is examined experimentally through “image analysis of liquid rising”. Additionally, the analysis of wicking in a single cotton fiber is done using an optical macroscopic method. Thereafter, a mathematical model for wicking in textile is developed based on textile structure and capillarity properties in macro- and microscales.

4. Wicking characterization of the liquid on or in the cellulosic fibers is carried out using confocal laser scanning microscopy. Fluorescent beads having various sizes in the micro- and nano range are flown along the fibers to investigate channel size at different scales. Time-lapse imaging is carried out to measure wicking rate, while z-stacking imaging is conducted to know the exact wicking position in the fiber.
5. Several low-cost health care devices based on natural cellulosic fibers are developed by inspiration from the wicking and wetting properties of natural cellulose fibers.

1.6 Thesis outline

Remaining chapters of thesis are organized as follows (Figure 1.1);

Chapter 2 presents the main concept of microfluidics in order to introduce the physical aspect behind microfluidics. It introduces to explain the chemical and the physical properties of single natural cellulose fiber such as cotton and kapok fibers. In the final section of this chapter, research on analytical analysis of liquid transport through fabric structures will be reviewed.

Chapter 3 conveys details for investigation of the physical properties of natural cellulose fibers to achieve appropriate understandings of the wicking flow through the hierarchical structures of natural cellulose fibers and cotton fabric.

Chapter 4, 5 and 6 explain several implementations of the wicking study to develop fiber-based biodiagnostic devices for point of care applications. The steps and procedures for the fabrication and development of fabric and thread based microfluidic for the cells sorting will be explained in chapters 4 and 5, respectively. Chapter 6 will present the development of fiber-based CRP-ELISA to detect the

salivary C-reactive protein (CRP) level as a predictor for cardiovascular disease (CVD).

Chapter 7 concludes the whole research approach and give some suggestions for further study.

It should be noted that chapters 3 to 6 have been written as separate journal papers, which have been submitted to or are already accepted for scientific journal publications. A list of publication is given in Appendix A.

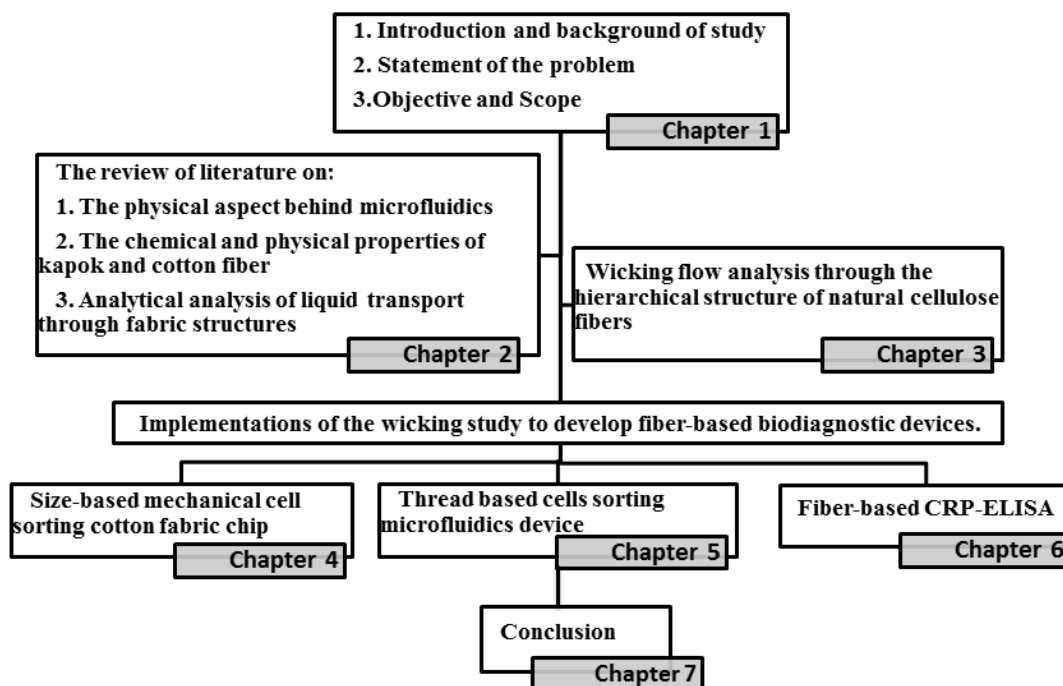


Figure 1.1; Flowchart representation of the thesis structure

REFERENCES

1. Gravesen, P., J. Branebjerg and O. S. Jensen. Microfluidics - a review. *Journal of Micromechanics and Microengineering*. 1993. 3(4): 168-182.
2. Park, J. M., A. T. Evans, K. Rasmussen, T. R. Brosten, *et al.* A microvalve with integrated sensors and customizable normal state for low-temperature operation. *Journal of Microelectromechanical Systems*. 2009. 18(4): 868-877.
3. Zhang, W., S. Lin, C. Wang, J. Hu, *et al.* PMMA/PDMS valves and pumps for disposable microfluidics. *Lab on a Chip - Miniaturisation for Chemistry and Biology*. 2009. 9(21): 3088-3094.
4. Zhu, Z., Z. F. Zhou, Q. A. Huang and W. H. Li. Modeling, simulation and experimental verification of inclined UV lithography for SU-8 negative thick photoresists. *Journal of Micromechanics and Microengineering*. 2008. 18(12).
5. Bruzewicz, D. A., M. Reches and G. M. Whitesides. Low-cost printing of poly(dimethylsiloxane) barriers to define microchannels in paper. *Analytical Chemistry*. 2008. 80(9): 3387-3392.
6. Weibel, D. B., M. Kruithof, S. Potenta, S. K. Sia, *et al.* Torque-actuated valves for microfluidics. *Analytical Chemistry*. 2005. 77(15): 4726-4733.
7. Martinez, A. W., S. T. Phillips and G. M. Whitesides. Three-dimensional microfluidic devices fabricated in layered paper and tape. *Proceedings of the National Academy of Sciences of the United States of America*. 2008. 105(50): 19606-19611.
8. Martinez, A. W., S. T. Phillips, G. M. Whitesides and E. Carrilho. Diagnostics for the developing world: Microfluidic paper-based analytical devices. *Analytical Chemistry*. 2010. 82(1): 3-10.
9. Li, X., J. Tian and W. Shen. Thread as a versatile material for low-cost microfluidic diagnostics. *ACS Applied Materials and Interfaces*. 2010. 2(1): 1-6.

10. Reches, M., K. A. Mirica, R. Dasgupta, M. D. Dickey, *et al.* Thread as a Matrix for Biomedical Assays. *ACS Applied Materials and Interfaces*. 2010. 2(6): 1722-1728.
11. Bhandari, P., T. Narahari and D. Dendukuri. Fab-Chips: A versatile, fabric-based platform for low-cost, rapid and multiplexed diagnostics. *Lab on a Chip - Miniaturisation for Chemistry and Biology*. 2011. 11(15): 2493-2499.
12. Nilghaz, A., D. H. B. Wicaksono, D. Gustiono, F. A. Abdul Majid, *et al.* Flexible microfluidic cloth-based analytical devices using a low-cost wax patterning technique. *Lab on a Chip*. 2012.
13. Huang, W., Q. Liu and Y. Li. Capillary Filling Flows inside Patterned-Surface Microchannels. *Chemical Engineering & Technology*. 2006. 29(6): 716-723.
14. Bouaidat, S., O. Hansen, H. Bruus, C. Berendsen, *et al.* Surface-directed capillary system; theory, experiments and applications. *Lab on a Chip - Miniaturisation for Chemistry and Biology*. 2005. 5(8): 827-836.
15. Juncker, D., H. Schmid, U. Drechsler, H. Wolf, *et al.* Autonomous microfluidic capillary system. *Analytical Chemistry*. 2002. 74(24): 6139-6144.
16. Zimmermann, M., P. Hunziker and E. Delamarche. Valves for autonomous capillary systems. *Microfluidics and Nanofluidics*. 2008. 5(3): 395-402.
17. Zimmermann, M., H. Schmid, P. Hunziker and E. Delamarche. Capillary pumps for autonomous capillary systems. *Lab on a Chip - Miniaturisation for Chemistry and Biology*. 2007. 7(1): 119-125.
18. Carrilho, E., A. W. Martinez and G. M. Whitesides. Understanding Wax Printing: A Simple Micropatterning Process for Paper-Based Microfluidics. *Analytical Chemistry*. 2009. 81(16): 7091-7095.
19. Dungchai, W., O. Chailapakul and C. S. Henry. A low-cost, simple, and rapid fabrication method for paper-based microfluidics using wax screen-printing. *Analyst*. 2011. 136(1): 77-82.
20. Olkkonen, J., K. Lehtinen and T. Erho. Flexographically Printed Fluidic Structures in Paper. *Analytical Chemistry*. 2010. 82(24): 10246-10250.

21. Li, X., J. Tian, G. Garnier and W. Shen. Fabrication of paper-based microfluidic sensors by printing. *Colloids and Surfaces B: Biointerfaces*. 2010. 76(2): 564-570.
22. Deiss, F., A. Mazzeo, E. Hong, D. E. Ingber, *et al.* Platform for High-Throughput Testing of the Effect of Soluble Compounds on 3D Cell Cultures. *Analytical Chemistry*. 2013. 85(17): 8085-8094.
23. Li, X., J. Tian, T. Nguyen and W. Shen. Paper-Based Microfluidic Devices by Plasma Treatment. *Analytical Chemistry*. 2008. 80(23): 9131-9134.
24. Chitnis, G., Z. Ding, C.-L. Chang, C. A. Savran, *et al.* Laser-treated hydrophobic paper: an inexpensive microfluidic platform. *Lab on a Chip*. 2011. 11(6): 1161-1165.
25. Abe, K., K. Suzuki and D. Citterio. Inkjet-Printed Microfluidic Multianalyte Chemical Sensing Paper. *Analytical Chemistry*. 2008. 80(18): 6928-6934.
26. Pelton, R. Bioactive paper provides a low-cost platform for diagnostics. *TrAC Trends in Analytical Chemistry*. 2009. 28(8): 925-942.
27. Ballerini, D. R., X. Li and W. Shen. Patterned paper and alternative materials as substrates for low-cost microfluidic diagnostics. *Microfluidics and nanofluidics*. 2012. 13(5): 769-787.
28. Nilghaz, A., D. H. Wicaksono, D. Gustiono, F. A. A. Majid, *et al.* Flexible microfluidic cloth-based analytical devices using a low-cost wax patterning technique. *Lab on a Chip*. 2012. 12(1): 209-218.
29. Reches, M. Thread Based Devices for Low-Cost Diagnostics. *Microfluidic Diagnostics*. Springer. 197-205; 2013
30. Ballerini, D. R., X. Li and W. Shen. An inexpensive thread-based system for simple and rapid blood grouping. *Analytical and bioanalytical chemistry*. 2011. 399(5): 1869-1875.
31. Bagherbaigi, S., E. P. Corcoles and D. H. B. Wicaksono. Cotton fabric as an immobilization matrix for low-cost and quick colorimetric enzyme-linked immunosorbent assay (ELISA). *Analytical Methods*. 2014.
32. Malon, R. S. P., K. Y. Chua, D. H. B. Wicaksono and E. P. Corcoles. Cotton fabric-based electrochemical device for lactate measurement in saliva. *Analyst*. 2014. 139(12): 3009-3016.

33. Yuen, A.-C., A. Bakir, N. Rajdi, C. L. Lam, *et al.* Proprioceptive Sensing System for Therapy Assessment Using Cotton Fabric-Based Biomedical Micro Electro Mechanical System. 2014.
34. Safavieh, R., G. Z. Zhou and D. Juncker. Microfluidics made of yarns and knots: from fundamental properties to simple networks and operations. *Lab on a Chip*. 2011. 11(15): 2618-2624.
35. Bhandari, P., T. Narahari and D. Dendukuri. 'Fab-Chips': a versatile, fabric-based platform for low-cost, rapid and multiplexed diagnostics. *Lab on a Chip*. 2011. 11(15): 2493-2499.
36. Prakash, S. and J. Yeom. *Nanofluidics and Microfluidics: Systems and Applications*: William Andrew. 2014
37. Mirasoli, M., M. Guardigli, E. Michelini and A. Roda. Recent advancements in chemical luminescence-based lab-on-chip and microfluidic platforms for bioanalysis. *Journal of pharmaceutical and biomedical analysis*. 2014. 87: 36-52.
38. Squires, T. M. and S. R. Quake. Microfluidics: Fluid physics at the nanoliter scale. *Reviews of modern physics*. 2005. 77(3): 977.
39. Khan, W. A. and M. M. Yovanovich. Analytical modeling of fluid flow and heat transfer in microchannel/nanochannel heat sinks. *Journal of Thermophysics and Heat Transfer*. 2008. 22(3): 352-359.
40. Blankenstein, G., Micro-flow system for particle separation and analysis. 2002, Google Patents.
41. Beebe, D. J., G. A. Mensing and G. M. Walker. Physics and applications of microfluidics in biology. *Annual review of biomedical engineering*. 2002. 4(1): 261-286.
42. Weibel, D. B. and G. M. Whitesides. Applications of microfluidics in chemical biology. *Current opinion in chemical biology*. 2006. 10(6): 584-591.
43. Andersson, H. and A. Van den Berg. Microfluidic devices for cellomics: a review. *Sensors and Actuators B: Chemical*. 2003. 92(3): 315-325.
44. Hänggi, P. and F. Marchesoni. Artificial Brownian motors: Controlling transport on the nanoscale. *Reviews of Modern Physics*. 2009. 81(1): 387.

45. Dreher, S., N. Kockmann and P. Woias. Characterization of laminar transient flow regimes and mixing in T-shaped micromixers. *Heat Transfer Engineering*. 2009. 30(1-2): 91-100.
46. Kwapiszewski, R., K. Ziolkowska, K. Zukowski, M. Chudy, *et al.* Effect of a high surface-to-volume ratio on fluorescence-based assays. *Analytical and bioanalytical chemistry*. 2012. 403(1): 151-155.
47. Carré, A. and K. L. Mittal. *Superhydrophobic surfaces*: Brill. 2009
48. Yuan, Y. and T. R. Lee. Contact angle and wetting properties. *Surface Science Techniques*. Springer. 3-34; 2013
49. Israelachvili, J. N. *Intermolecular and surface forces: revised third edition*: Academic press. 2011
50. Orwell, R. M. H., James S. and Rowell, Jeffrey S. . Characterization and Factors Effecting Fiber Properties. . *Natural Polymers and Argo-fibers Composites* São Carlos - Brazil.
51. Morton, W. E., J. W. S. Hearle and T. Institute. *Physical properties of textile fibres*: Woodhead Publishing in association with the Textile Institute. 2008
52. Akasheh, F., H. M. Zbib, S. Akarapu, C. Overman, *et al.* Multiscale modeling of dislocation mechanisms in nanoscale multilayered composites. 2008. 7-12.
53. Hearle, J. W. S. The structural mechanics of fibers. *Journal of Polymer Science Part C: Polymer Symposia*. 1967. 20(1): 215-251.
54. Fan, Q. *Chemical Testing of Textiles*: CRC Press. 2005
55. Militký, J., I. Sayed, Y. Demet and F. Goktepe. Bimodality of the cotton compact yarn hairiness index. *Izvestiya Vysshikh Uchebnykh Zavedenii, Seriya Tekhnologiya Tekstil'noi Promyshlennosti*. 2009(3 C): 34-39.
56. Das, D. B., M. K. Mitra and J. F. Wareham. Structure of cotton alpha-cellulose. *Nature*. 1954. 174(4440): 1058-1059.
57. Adams, G. A. and C. T. Bishop. Polysaccharides associated with alpha-cellulose [2]. *Nature*. 1953. 172(4366): 28-29.
58. Gordon, S. and Y. Hsieh. *Cotton: science and technology*: Woodhead. 2007
59. Mangat, M. M. A. Structure and Properties of Cotton Fiber. 2009.
60. Phillip J . Wakelyn , N. R. B., Alfred Dexter French , Devron P . Thibodeaux , Marie-Alice Rousselle , Barbara A . Triplett , Wilton R . Goynes , J . Vincent Edwards , Lawrance Hunter , David D . McAlister , and Gary R .

- Gamble. Structural Properties of Cotton. *Cotton Fiber Chemistry and Technology*. CRC Press. 2007
61. Mhetre, S. and R. Parachuru. The effect of fabric structure and yarn-to-yarn liquid migration on liquid transport in fabrics. *The Journal of the Textile Institute*. 2010. 101(7): 621-626.
 62. Rengasamy, R., D. Das and C. Praba Karan. Study of oil sorption behavior of filled and structured fiber assemblies made from polypropylene, kapok and milkweed fibers. *Journal of hazardous materials*. 2011. 186(1): 526-532.
 63. Tye, Y. Y., K. T. Lee, W. N. Wan Abdullah and C. P. Leh. Potential of *Ceiba pentandra* (L.) Gaertn. (kapok fiber) as a resource for second generation bioethanol: Effect of various simple pretreatment methods on sugar production. *Bioresource technology*. 2012. 116: 536-539.
 64. Lim, T.-T. and X. Huang. Evaluation of kapok (*Ceiba pentandra* (L.) Gaertn.) as a natural hollow hydrophobic–oleophilic fibrous sorbent for oil spill cleanup. *Chemosphere*. 2007. 66(5): 955-963.
 65. Hori, K., M. Flavier, S. Kuga, T. Lam, *et al.* Excellent oil absorbent kapok [*Ceiba pentandra* (L.) Gaertn.] fiber: fiber structure, chemical characteristics, and application. *Journal of Wood Science*. 2000. 46(5): 401-404.
 66. Rijavec, T. Kapok in technical textiles. *Tekstilec*. 2008. 51(10-12): 319-331.
 67. Liu, Y., J. Wang, Y. Zheng and A. Wang. Adsorption of methylene blue by kapok fiber treated by sodium chlorite optimized with response surface methodology. *Chemical Engineering Journal*. 2012. 184(0): 248-255.
 68. Mwaikambo, L. Y. and M. P. Ansell. The effect of chemical treatment on the properties of hemp, sisal, jute and kapok fibres for composite reinforcement. *Die angewandte makromolekulare Chemie*. 1999. 272(1): 108-116.
 69. Hollies, N. R. S., M. M. Kaessinger, B. S. Watson and H. Bogaty. Water Transport Mechanisms in Textile Materials. *Textile Research Journal*. 1957. 27(1): 8-13.
 70. Minor, F. M., & Schwartz, A.M. Pathways of capillary migration of liquids in textile assemblies. *American Dyestuff Reporter*. 1960. 49: 37-42.

71. Marmur, A. and R. D. Cohen. Characterization of porous media by the kinetics of liquid penetration: The vertical capillaries model. *Journal of Colloid and Interface Science*. 1997. 189(2): 299-304.
72. Ichikawa, N. and Y. Satoda. Interface Dynamics of Capillary Flow in a Tube under Negligible Gravity Condition. *Journal of Colloid and Interface Science*. 1994. 162(2): 350-355.
73. Lu, W.-M., K.-L. Tung and K.-J. Hwang. Fluid Flow Through Basic Weaves of Monofilament Filter Cloth. *Textile Research Journal*. 1996. 66(5): 311-323.
74. Perwuelz, A., P. Mondon and C. Caze. Experimental Study of Capillary Flow in Yarns. *Textile Research Journal*. 2000. 70(4): 333-339.
75. Rajagopalan, D., A. P. Aneja and J.-M. Marchal. Modeling Capillary Flow in Complex Geometries. *Textile Research Journal*. 2001. 71(9): 813-821.
76. Patnaik, A., a. Ghosh, T. Institute and R. S. Rengasamy. *Wetting and Wicking in Fibrous Materials*: Woodhead Pub Ltd. 2006
77. Das, B., A. Das, V. K. Kothari and R. Figueiro. Development of mathematical model to predict vertical wicking behaviour. part I: flow through yarn. *Journal of the Textile Institute*. 2011. 102(11): 957-970.
78. Miller, B. and D. B. Clark. Liquid Transport Through Fabrics; Wetting and Steady-State Flow Part I: A New Experimental Approach. *Textile Research Journal*. 1978. 48(3): 150-155.
79. Yu, B. and L. James Lee. A simplified in-plane permeability model for textile fabrics. *Polymer Composites*. 2000. 21(5): 660-685.
80. Das, B., A. Das, V. K. Kothari and R. Figueiro. Mathematical model to predict vertical wicking behaviour. part ii: flow through woven fabric. *Journal of the Textile Institute*. 2011. 102(11): 971-981.
81. Ludwig, R. Chapter VI Fibers and fibrous materials. In: P. K. Chatterjee and B. S. Gupta. eds. *Textile Science and Technology*. Elsevier. 199-232; 2002
82. Chatterjee, P. K. *Absorbency*: Elsevier Scientific Pub. 1985
83. Bruus, H. *Theoretical microfluidics*: Oxford University Press. 2008
84. Kissa, E. Wetting and wicking. *Textile Research Journal*. 1996. 66(10): 660-668.

85. Hsieh, Y.-L., A. Miller and J. Thompson. Wetting, pore structure, and liquid retention of hydrolyzed polyester fabrics. *Textile research journal*. 1996. 66(1): 1-10.
86. Kim, J. Y. and D. Y. Lim. Surface-modified membrane as a separator for lithium-ion polymer battery. *Energies*. 2010. 3(4): 866-885.
87. Karmakar, S. R. *Chemical technology in the pre-treatment processes of textiles*, ed. Vol. 12: Elsevier. 1999
88. Mohanty, A. K., M. Misra and L. T. Drzal. *Natural Fibers, Biopolymers, and Biocomposites*: Taylor & Francis. 2005
89. Li, X., L. G. Tabil and S. Panigrahi. Chemical treatments of natural fiber for use in natural fiber-reinforced composites: a review. *Journal of Polymers and the Environment*. 2007. 15(1): 25-33.
90. Suter, S. P. and R. Skalak. The history of Poiseuille's law. *Annual Review of Fluid Mechanics*. 1993. 25(1): 1-20.
91. Kosek, J., F. Štěpánek and M. Marek. Modeling of transport and transformation processes in porous and multiphase bodies. *Advances in chemical engineering*. 2005. 30: 137-203.
92. Happel, J. and H. Brenner. *Low Reynolds number hydrodynamics: with special applications to particulate media*, ed. Vol. 1: Springer. 1983
93. Teeri, T. T., H. Brumer III, G. Daniel and P. Gatenholm. Biomimetic engineering of cellulose-based materials. *TRENDS in Biotechnology*. 2007. 25(7): 299-306.
94. Wang, J. and A. Wang. Acetylated modification of kapok fiber and application for oil absorption. *Fibers and Polymers*. 2013. 14(11): 1834-1840.
95. Hou, Y., Y. Chen, Y. Xue, L. Wang, *et al.* Stronger water hanging ability and higher water collection efficiency of bioinspired fiber with multi-gradient and multi-scale spindle knots. *Soft Matter*. 2012. 8(44): 11236-11239.
96. Drummond, J. and M. Tahir. Laminar viscous flow through regular arrays of parallel solid cylinders. *International Journal of Multiphase Flow*. 1984. 10(5): 515-540.

97. Su, X., A. B. Theberge, C. T. January and D. J. Beebe. Effect of Microculture on Cell Metabolism and Biochemistry: Do Cells Get Stressed in Microchannels? *Analytical Chemistry*. 2013. 85(3): 1562-1570.
98. Osborn, J. L., B. Lutz, E. Fu, P. Kauffman, *et al.* Microfluidics without pumps: reinventing the T-sensor and H-filter in paper networks. *Lab on a Chip*. 2010. 10(20): 2659-2665.
99. Fiorini, G. S. and D. T. Chiu. Disposable microfluidic devices: fabrication, function, and application. *BioTechniques*. 2005. 38(3): 429-446.
100. Gardeniersab, J., R. Oosterbroekb and A. van den Berg. Silicon and glass micromachining for jiTAS. *Lab-on-a-Chip: Miniaturized Systems for (Bio) Chemical Analysis and Synthesis*. 2003: 37.
101. Sharma, H., D. Nguyen, A. Chen, V. Lew, *et al.* Unconventional low-cost fabrication and patterning techniques for point of care diagnostics. *Annals of biomedical engineering*. 2011. 39(4): 1313-1327.
102. El-Ali, J., P. K. Sorger and K. F. Jensen. Cells on chips. *Nature*. 2006. 442(7101): 403-411.
103. Yun, H., K. Kim and W. G. Lee. Cell manipulation in microfluidics. *Biofabrication*. 2013. 5(2): 022001.
104. Fiedler, S., S. G. Shirley, T. Schnelle and G. Fuhr. Dielectrophoretic sorting of particles and cells in a microsystem. *Analytical Chemistry*. 1998. 70(9): 1909-1915.
105. Wang, M. M., E. Tu, D. E. Raymond, J. M. Yang, *et al.* Microfluidic sorting of mammalian cells by optical force switching. *Nature biotechnology*. 2004. 23(1): 83-87.
106. Dittrich, P. S., K. Tachikawa and A. Manz. Micro total analysis systems. Latest advancements and trends. *Analytical Chemistry*. 2006. 78(12): 3887-3908.
107. Miltenyi, S., W. Müller, W. Weichel and A. Radbruch. High gradient magnetic cell separation with MACS. *Cytometry*. 1990. 11(2): 231-238.
108. Bhagat, A. A. S., H. W. Hou, L. D. Li, C. T. Lim, *et al.* Pinched flow coupled shear-modulated inertial microfluidics for high-throughput rare blood cell separation. *Lab on a Chip*. 2011. 11(11): 1870-1878.

109. Yao, B., G.-a. Luo, X. Feng, W. Wang, *et al.* A microfluidic device based on gravity and electric force driving for flow cytometry and fluorescence activated cell sorting. *Lab Chip*. 2004. 4(6): 603-607.
110. Gossett, D. R., W. M. Weaver, A. J. Mach, S. C. Hur, *et al.* Label-free cell separation and sorting in microfluidic systems. *Analytical and bioanalytical chemistry*. 2010. 397(8): 3249-3267.
111. Nge, P. N., C. I. Rogers and A. T. Woolley. Advances in microfluidic materials, functions, integration, and applications. *Chemical reviews*. 2013. 113(4): 2550-2583.
112. Freshney, R. I. *Culture of specific cell types*: Wiley Online Library. 2005
113. Kvam, E. and R. M. Tyrrell. Induction of oxidative DNA base damage in human skin cells by UV and near visible radiation. *Carcinogenesis*. 1997. 18(12): 2379-2384.
114. Nyoni, A. and D. Brook. Wicking mechanisms in yarns—the key to fabric wicking performance. *Journal of the Textile Institute*. 2006. 97(2): 119-128.
115. Flemming, R., C. Murphy, G. Abrams, S. Goodman, *et al.* Effects of synthetic micro-and nano-structured surfaces on cell behavior. *Biomaterials*. 1999. 20(6): 573-588.
116. Kirschner, C. M., J. F. Schumacher and A. B. Brennan. Cellular Responses to Bio-Inspired Engineered Topography. *Bio-inspired Materials for Biomedical Engineering*. 2014: 77-97.
117. Chatterjee, A. and P. Singh. Studies on Wicking Behaviour of Polyester Fabric. *Journal of Textiles*. 2014. 2014.
118. Benltoufa, S., F. Fayala and S. BenNasrallah. Capillary rise in macro and micro pores of jersey knitting structure. *Journal of Engineered Fibers and Fabrics (JEFF)*. 2008. 3(3): 47-54.
119. Bertoniere, N. R. and W. D. King. Effect of scouring/bleaching, caustic mercerization, and liquid ammonia treatment on the pore structure of cotton textile fibers. *Textile Research Journal*. 1989. 59(2): 114-121.
120. Chen, X., On-chip pretreatment of whole blood by using mems technology, X. Chen, Editor. 2010, Bentham Science: Dubai, U.A.E. p. 27.
121. Kim, S. M., S. H. Lee and K. Y. Suh. Cell research with physically modified microfluidic channels: a review. *Lab Chip*. 2008. 8(7): 9.

122. Choi, S., S. Song, C. Choi and J. K. Park. Continuous blood cell separation by hydrophoretic filtration. *Lab on a Chip*. 2007. 7: 7.
123. Carroll, R. J. and W. C. Smith, Method of using anticoagulant solution in blood separation. 1996, Google Patents.
124. Ballerini, D. R., X. Li and W. Shen. Flow control concepts for thread-based microfluidic devices. *Biomicrofluidics*. 2011. 5(1): 014105.
125. Green, A., D. Powe, E. Rakha, D. Soria, *et al.* Identification of key clinical phenotypes of breast cancer using a reduced panel of protein biomarkers. *British journal of cancer*. 2013. 109(7): 1886-1894.
126. Pin, E., C. Fredolini and E. F. Petricoin III. The role of proteomics in prostate cancer research: Biomarker discovery and validation. *Clinical biochemistry*. 2013. 46(6): 524-538.
127. Zhang, Z., R. C. Bast, Y. Yu, J. Li, *et al.* Three biomarkers identified from serum proteomic analysis for the detection of early stage ovarian cancer. *Cancer research*. 2004. 64(16): 5882-5890.
128. Christodoulides, N., F. N. Pierre, X. Sanchez, L. Li, *et al.* Programmable Bio-Nano-Chip Technology for the Diagnosis of Cardiovascular Disease at the Point-of-Care. *Methodist DeBakey cardiovascular journal*. 2012. 8(1): 6.
129. Hojatollah, Y. Relation of Saliva and Blood Troponin Levels in Patients with Myocardial Infarction: Cross-Sectional Clinical Study. *International Journal of Cardiovascular Research*. 2012.
130. Blennow, K. Cerebrospinal fluid protein biomarkers for Alzheimer's disease. *NeuroRx*. 2004. 1(2): 213-225.
131. Diamandis, E. P. Mass spectrometry as a diagnostic and a cancer biomarker discovery tool opportunities and potential limitations. *Molecular & Cellular Proteomics*. 2004. 3(4): 367-378.
132. McDonagh, B., R. Tyther and D. Sheehan. Carbonylation and glutathionylation of proteins in the blue mussel *Mytilus edulis* detected by proteomic analysis and Western blotting: Actin as a target for oxidative stress. *Aquatic Toxicology*. 2005. 73(3): 315-326.
133. Gygi, S. P., G. L. Corthals, Y. Zhang, Y. Rochon, *et al.* Evaluation of two-dimensional gel electrophoresis-based proteome analysis technology. *Proceedings of the National Academy of Sciences*. 2000. 97(17): 9390-9395.

134. Rusling, J. F., C. V. Kumar, J. S. Gutkind and V. Patel. Measurement of biomarker proteins for point-of-care early detection and monitoring of cancer. *Analyst*. 2010. 135(10): 2496-2511.
135. Liuzzo, G., L. M. Biasucci, J. R. Gallimore, R. L. Grillo, *et al.* The prognostic value of C-reactive protein and serum amyloid a protein in severe unstable angina. *New England journal of medicine*. 1994. 331(7): 417-424.
136. McConnell, J. P., E. L. Branum, K. V. Ballman, S. A. Lagerstedt, *et al.* Gender differences in C-reactive protein concentrations-confirmation with two sensitive methods. *Clinical chemistry and laboratory medicine*. 2002. 40(1): 56-59.
137. Chul Sung, K., J. Y. Suh, B. S. Kim, J. H. Kang, *et al.* High sensitivity C-reactive protein as an independent risk factor for essential hypertension. *American journal of hypertension*. 2003. 16(6): 429-433.
138. Fan, Z., Y. S. Keum, Q. X. Li, W. L. Shelver, *et al.* Sensitive immunoassay detection of multiple environmental chemicals on protein microarrays using DNA/dye conjugate as a fluorescent label. *Journal of Environmental Monitoring*. 2012. 14(5): 1345-1352.
139. Ellerbee, A. K., S. T. Phillips, A. C. Siegel, K. A. Mirica, *et al.* Quantifying colorimetric assays in paper-based microfluidic devices by measuring the transmission of light through paper. *Analytical chemistry*. 2009. 81(20): 8447-8452.
140. Zou, Z., D. Du, J. Wang, J. N. Smith, *et al.* Quantum dot-based immunochromatographic fluorescent biosensor for biomonitoring trichloropyridinol, a biomarker of exposure to chlorpyrifos. *Analytical chemistry*. 2010. 82(12): 5125-5133.
141. Elenis, D. S., P. C. Ioannou and T. K. Christopoulos. Quadruple-analyte chemiluminometric hybridization assay. Application to double quantitative competitive polymerase chain reaction. *Analytical chemistry*. 2007. 79(24): 9433-9440.
142. Lin, K.-C., V. Kunduru, M. Bothara, K. Rege, *et al.* Biogenic nanoporous silica-based sensor for enhanced electrochemical detection of cardiovascular biomarkers proteins. *Biosensors and Bioelectronics*. 2010. 25(10): 2336-2342.

143. Lenshof, A., A. Ahmad-Tajudin, K. Järås, A.-M. Swärd-Nilsson, *et al.* Acoustic whole blood plasmapheresis chip for prostate specific antigen microarray diagnostics. *Analytical chemistry*. 2009. 81(15): 6030-6037.
144. Ling, Y., T. Pong, C. C. Vassiliou, P. L. Huang, *et al.* Implantable magnetic relaxation sensors measure cumulative exposure to cardiac biomarkers. *Nature biotechnology*. 2011. 29(3): 273-277.
145. Rosi, N. L. and C. A. Mirkin. Nanostructures in biodiagnostics. *Chemical reviews*. 2005. 105(4): 1547-1562.
146. Stoeva, S. I., J.-S. Lee, J. E. Smith, S. T. Rosen, *et al.* Multiplexed detection of protein cancer markers with biobarcode nanoparticle probes. *Journal of the American Chemical Society*. 2006. 128(26): 8378-8379.
147. Chen, H., C. Jiang, C. Yu, S. Zhang, *et al.* Protein chips and nanomaterials for application in tumor marker immunoassays. *Biosensors and Bioelectronics*. 2009. 24(12): 3399-3411.
148. Tsou, P., C. Chou, S. Saldana, M. Hung, *et al.* The fabrication and testing of electrospun silica nanofiber membranes for the detection of proteins. *Nanotechnology*. 2008. 19(44): 445714.
149. Cheng, C. M., A. W. Martinez, J. Gong, C. R. Mace, *et al.* Paper-Based ELISA. *Angewandte Chemie International Edition*. 2010. 49(28): 4771-4774.
150. Zhou, G., X. Mao and D. Juncker. Immunochromatographic assay on thread. *Analytical chemistry*. 2012. 84(18): 7736-7743.
151. Pearson, T. A., G. A. Mensah, R. W. Alexander, J. L. Anderson, *et al.* Markers of inflammation and cardiovascular disease application to clinical and public health practice: a statement for healthcare professionals from the centers for disease control and prevention and the American Heart Association. *Circulation*. 2003. 107(3): 499-511.
152. Li, J.-J. and C.-H. Fang. C-reactive protein is not only an inflammatory marker but also a direct cause of cardiovascular diseases. *Medical hypotheses*. 2004. 62(4): 499-506.
153. Willerson, J. T. and P. M. Ridker. Inflammation as a cardiovascular risk factor. *Circulation*. 2004. 109(21 suppl 1): II-2-II-10.

154. Brodin, F. W. and H. Theliander. Absorbent materials based on kraft pulp: Preparation and material characterization. *BioResources*. 2012. 7(2): 1666-1683.
155. Grinnell, F. and M. Feld. Fibronectin adsorption on hydrophilic and hydrophobic surfaces detected by antibody binding and analyzed during cell adhesion in serum-containing medium. *Journal of Biological Chemistry*. 1982. 257(9): 4888-4893.
156. Nakanishi, K., T. Sakiyama and K. Imamura. On the adsorption of proteins on solid surfaces, a common but very complicated phenomenon. *Journal of Bioscience and Bioengineering*. 2001. 91(3): 233-244.
157. Krishnan, A., P. Cha, Y.-H. Liu, D. Allara, *et al.* Interfacial energetics of blood plasma and serum adsorption to a hydrophobic self-assembled monolayer surface. *Biomaterials*. 2006. 27(17): 3187-3194.
158. Abdul Khalil, H., A. Bhat and A. Ireana Yusra. Green composites from sustainable cellulose nanofibrils: a review. *Carbohydrate Polymers*. 2012. 87(2): 963-979.
159. Findlay, J. W. and R. F. Dillard. Appropriate calibration curve fitting in ligand binding assays. *The AAPS journal*. 2007. 9(2): E260-E267.
160. Weinrich, D., P. Jonkheijm, C. M. Niemeyer and H. Waldmann. Applications of protein biochips in biomedical and biotechnological research. *Angewandte Chemie International Edition*. 2009. 48(42): 7744-7751.
161. Aussawasathien, D., P. He and L. Dai. Polymer nanofibers and polymer sheathed carbon nanotubes for sensors. *ACS Symposium series*: Oxford University Press. 2006. 246-268.
162. Christodoulides, N., S. Mohanty, C. S. Miller, M. C. Langub, *et al.* Application of microchip assay system for the measurement of C-reactive protein in human saliva. *Lab on a Chip*. 2005. 5(3): 261-269.
163. Haynes, C. A. and W. Norde. Structures and stabilities of adsorbed proteins. *Journal of Colloid and Interface Science*. 1995. 169(2): 313-328.
164. Krishnan, A. *Protein Adsorption to Hydrophobic Surfaces*. The Pennsylvania State University; 2005

165. Lee, Y.-H., D. T. Wong, Y. Lee and D. Wong. Saliva: an emerging biofluid for early detection of diseases. *American journal of dentistry*. 2009. 22(4): 241.
166. Gilman, F. J. and M. B. Wise. Effective Hamiltonian for $\Delta S=1$ weak nonleptonic decays in the six-quark model. *Physical Review D*. 1979. 20(9): 2392.
167. Bosch, J. A., H. S. Brand, T. Ligtenberg, B. Bermond, *et al.* Psychological stress as a determinant of protein levels and salivary-induced aggregation of *Streptococcus gordonii* in human whole saliva. *Psychosomatic medicine*. 1996. 58(4): 374-382.
168. Nater, U. and N. Rohleder. Salivary alpha-amylase as a non-invasive biomarker for the sympathetic nervous system: current state of research. *Psychoneuroendocrinology*. 2009. 34(4): 486-496.
169. van Stegeren, A., N. Rohleder, W. Everaerd and O. T. Wolf. Salivary alpha amylase as marker for adrenergic activity during stress: effect of betablockade. *Psychoneuroendocrinology*. 2006. 31(1): 137-141.
170. Bernfeld, P. [17] Amylases, α and β . *Methods in enzymology*. 1955. 1: 149-158.
171. Tlili, C., L. N. Cella, N. V. Myung, V. Shetty, *et al.* Single-walled carbon nanotube chemoresistive label-free immunosensor for salivary stress biomarkers. *Analyst*. 2010. 135(10): 2637-2642.
172. Shetty, V., C. Zigler, T. F. Robles, D. Elashoff, *et al.* Developmental validation of a point-of-care, salivary α -amylase biosensor. *Psychoneuroendocrinology*. 2011. 36(2): 193-199.
173. Gaillard, Y., J.-P. Gay-Montchamp and M. Ollagnier. Simultaneous screening and quantitation of alpidem, zolpidem, buspirone and benzodiazepines by dual-channel gas chromatography using electron-capture and nitrogen—phosphorus detection after solid-phase extraction. *Journal of Chromatography B: Biomedical Sciences and Applications*. 1993. 622(2): 197-208.
174. Takai, N., M. Yamaguchi, T. Aragaki, K. Eto, *et al.* Effect of psychological stress on the salivary cortisol and amylase levels in healthy young adults. *Archives of Oral Biology*. 2004. 49(12): 963-968.

175. Nater, U. M., R. La Marca, L. Florin, A. Moses, *et al.* Stress-induced changes in human salivary alpha-amylase activity—associations with adrenergic activity. *Psychoneuroendocrinology*. 2006. 31(1): 49-58.